



## Photocatalytic microbial removal and degradation of organic contaminants of water using PES fibers

Buthayna Al-Ghafri<sup>a</sup>, Tanujjal Bora<sup>a,b,\*</sup>, Priyanka Sathe<sup>a,c</sup>, Sergey Dobrestov<sup>c,d</sup>, Mohammed Al-Abri<sup>a,e,\*</sup>

<sup>a</sup> Nanotechnology Research Center, Sultan Qaboos University, PO Box 33, PC 123, Al-Khoudh, Oman

<sup>b</sup> Center of Excellence in Nanotechnology, Asian Institute of Technology, PO Box 4, Klong Luang, Pathumthani, 12120, Thailand

<sup>c</sup> Department of Marine Science & Fisheries, College of Agricultural & Marine Sciences, Sultan Qaboos University, PO Box 34, Al-Khoudh, Muscat 123, Oman

<sup>d</sup> Center of Excellence in Marine Biotechnology, Sultan Qaboos University, PO Box 50, Al-Khoudh, Muscat 123, Oman

<sup>e</sup> Department of Chemical and Petroleum Engineering, College of Engineering, Sultan Qaboos University, PO Box 33, PC 123, Al-Khoudh, Oman



### ARTICLE INFO

#### Keywords:

Polyethersulfone

Polymeric fiber

Photocatalysis

Water bacterial removal

Methylene blue

### ABSTRACT

Photocatalytic bacterial removal and dye degradation by polyethersulfone (PES) fibers under visible light is reported here. PES fibers were arranged in a random mesh structure using electro-spinning technique that allows utilization of maximum surface area of the fibers. The influence of concentration of PES polymer, type of solvent and surface chemistry of the fibers on their mechanical properties and photocatalytic activities was investigated. Ratio of solvent (DMF (Dimethylformamide) to NMP (N-Methyl-2-pyrrolidone)) while preparing the PES fibers was found to be crucial in terms of the PES fiber thickness, fluid flux, mechanical strength and hydrophobicity of the fibers. The as-prepared PES fibers showed considerable amount of OH<sup>·</sup> radical generation under visible light excitation resulting in efficient degradation of model dye contaminant methylene blue (MB) and disinfection of model bacterium *Escherichia coli* (*E. coli*). However increased hydrophilicity of the fibers using oxidation treatment resulted in reduction in the generation of OH<sup>·</sup> radicals showing less photocatalytic activity by the PES fibers. FTIR investigations confirmed no self-destruction of the PES fibers due to the generation OH<sup>·</sup> radicals indicating potential application of PES fibers as a useful photocatalytic polymer material for bacterial removal and decontamination of water.

### 1. Introduction

Recent scientific research on water treatment has emerging interest toward the uses of polymeric fiber membranes and modification of them to improve the filtration features at all different scales [1]. Polymeric fibers received a great deal of attention in water treatment because of their special features such as hydraulic permeability, mechanical strength and stability in required applications [2–4].

The key advantage of polymeric fiber membranes is their high selectivity for water components at different sizes during separation process which depends on the method of fabrication [5,6]. Moreover, polymeric membranes are fabricated in different filtration configurations and modules like reverse osmosis (RO), nanofiltration (NF), ultrafiltration (UF) and microfiltration (MF). Polymeric microfiltration membranes are widely used as pre-treatment in water filtration which can separate particles between 0.1 and 10 µm [6,7]. Polyethersulfone (PES) polymer has unique characteristics like thermal stability, heat

resistant and high pH resistance compared to other commonly used polymers in filtration application [6,8–10].

Mostly, microfiltration PES membrane is fabricated using Nanospinner instrument [11–13]. Nanospinner is a simple technique that applies electrostatic force to form fibers in nanometer size [6]. Several studies have mentioned that the average diameter of electro-spun nanofibers ranges from 100 nm to 500 nm and it is affected by several factors like polymer concentration, viscosity of solvents, flow rate of the solution, voltage used to create potential between collector and nozzle inside nanospinner, distance between collector and nozzle, rotation of the collector and humidity inside the nanospinner [14,15]. The exceptional features which make nanofibers extensively used in water treatment membrane is the uniform fibers, the small pore size between fibers network and the large surface area [6,16].

In general, electrospun PES fibers are hydrophobic and this limited their efficiency in water application because of low flux [17,18]. Furthermore, the performance of any membrane in terms of fouling,

\* Corresponding authors at: Nanotechnology Research Center, Sultan Qaboos University, PO Box 33, PC 123, Al-Khoudh, Oman.

E-mail addresses: [buthayna@graduate.utm.my](mailto:buthayna@graduate.utm.my) (B. Al-Ghafri), [tbora@ait.ac.th](mailto:tbora@ait.ac.th) (T. Bora), [P108960@squ.student.edu.om](mailto:P108960@squ.student.edu.om) (P. Sathe), [S. Dobrestov](mailto:Sergey@squ.edu.om), [alabri@squ.edu](mailto:alabri@squ.edu) (M. Al-Abri).

membrane rejection and permeate flux is affected by its level of hydrophobicity [19–21]. Several studies have had mentioned the methods used to reduce the hydrophobicity, which lead to increase the membrane's water applications [18,22]. For instance, inorganic nanoparticles such as metal oxides can reduce the hydrophobicity of the membrane [23]. On the other hand, hydrophilic membranes has a tendency to swell in water and thereby reducing their lifetime [24]. Consequently, a reduction in both mechanical strength of the membrane and rejections of particles happen [24,25].

Another obstacle that faces the water pre-treatment units is the membrane fouling, which is attachment and growth of microbial organisms, such as bacteria [26,27]. This process results in may results in pore blocking, adsorption of hydrophobic particles and nonpolar solutes, gel layer formation and cake layer formation [26]. Likewise, microbial bio-fouling results in shorter membrane lifetime [27].

To overcome the problem associated with membrane biofouling, bacterial removal of water by chlorine, ozone, silver nanoparticles [28] and metal oxide photocatalyst [29,30] are more common and have been used for various water applications [31,32]. Metals oxide have shown photocatalytic behaviour under light due to their wide gap energies [33]. The process of photocatalysis initiate when the light illumination is excited above band gap energy, generating exciton pairs. These photo-generated charges then interact with the surrounding and produce highly reactive species at the surface of photocatalyst that can break down organic contaminants and disinfect bacteria by oxidation or reduction process [34–36]. Similarly PES has also been reported to generate OH<sup>·</sup> radicals under visible light through various chemical reactions [37] giving these fibers self-cleaning properties. OH<sup>·</sup> is considered to be a strong oxidizing agent [38], consequently, it can be used efficiently for microbial removal [39].

For the best of our knowledge, the photocatalytic (PC) behavior of electrospun PES fibers has not been reported yet. This work addresses this issue and probe the formation of PES fibers network which are photocatalytic in nature. PES nanofibers were prepared by using Nanospinner and their photocatalytic activity was investigated using MB dye and *E. coli* bacterium as model contaminants. The fiber's properties were characterized using different techniques such as scanning electron microscope (SEM), Fourier transform infrared (FTIR), water contact angle (WCA) and mechanical strength measurements. Various factors, such as material concentration, surface chemistry and solvent types affecting the photocatalytic behaviour of the PES fibers have been studied and the possible mechanism behind the photocatalytic properties of PES fibers is discussed.

## 2. Experimental

### 2.1. Fabrication of PES nanofibres

PES (nominal granular size: 3 mm, from Goodfellow Cambridge limited company, PE29 6WR England, UK) was dissolve in *N*-methyl-pyrrolidinone (NMP) and Dimethylformamide (DMF, from Sigma-Aldrich) at certain volume ratio by mild stirring in oil bath (60 °C) for 48 h. Then the mixture was sonicated for another 40 min to ensure the complete dissolving of the polymer. Moreover, ammonium persulfate (APS, from Sigma-Aldrich) was used in some cases to reduce hydrophobicity of the fibers [25].

Multi nozzle Nanospinner (NS24) was used to prepare the PES fibers. Three different PES concentrations were tried (22%, 26%, and 28%) and the different volume ratios of DMF in NMP were used (1:1, 2:3, 7:3). During electrospinning process, all parameters were optimized. The feeding rate was fixed at 1.00 mL/h using syringe pump, the collector rotation speed was 220 rpm and the distance between the collector and the spinneret was optimized to be 130 cm. The prepared PES solutions were electrospun onto aluminium foil at a high voltage of 23.5 kV. After electrospun process, the PES meshes were air dried for 1 day and then easily removed from aluminium foil.

### 2.2. Characterization

Surface morphology of PES nanofibers was characterized by Field Emission Scanning Electron Microscope (Jeol JSM-7600F FESEM) operated at 20 kV. The fibers were dried completely in a desiccator and then coated with platinum to minimize the charging effect prior to carrying out SEM [29]. The fiber diameters were also measured from SEM images by using the Scion<sub>®</sub> image analysis program. To measure the mechanical strength of the fibers, Instron tensile machine (Tinius Olsen-H5KT) was used. The gauge length was 20 mm, the width at the centre was 20 mm, the specimen thickness was about 200 µm and the electrospun fibers piece was (2 cm × 2 cm). The results show force, the ultimate tensile strength and strain at break were measured, and Young's modulus was calculated. Moreover, Attenuated Total Reflection Fourier Transform Infrared (ATR-FTIR) was used to examine the surface groups of the PES fibers. To evaluate the electrospun PES surface hydrophobicity, water contact angle (WCA) was measured using One Attension program. Sessile drop method was used to get the angle using DI water with 5 µL as the probe liquid in five different places and then the average contact angle was calculated.

### 2.3. Photocatalytic tests

Methylene blue (MB) and the bacterium *E. coli* were used to study the photocatalytic activity of the PES fibers and all photocatalytic tests were conducted under visible light. MB with a concentration of 10 µM was prepared in DI water. A 30 mL of MB solution was kept in 100 mL beaker as a control, and same amount was added to the PES fibers (3 cm × 3 cm). The beakers were placed under visible light source using a solar simulator (AM 1.5 G radiation) equipped with IR filter to cut off any heat generated from the light source and the distance between the lamp and the beakers was adjusted so the light intensity is 1000 W/m<sup>2</sup> using a pyranometer (Iso-Tech ISM 410).

Approximately 1 mL of MB solution was taken as initial concentration (C<sub>0</sub>) at zero time and measured its absorbance using ocean optics program in the range of 500–760 nm in order to monitor the degradation of MB. Before starting the photocatalytic degradation test, both control and the membrane were kept in dark for 2 h to ensure that MB reach adsorption-desorption equilibrium with the PES fibers. Then, the optical absorption spectra were recorded at regular intervals in order to monitor the photocatalytic degradation spectra for MB by PES fibers. The absorption intensity of MB photo degradation was measured at  $\lambda_{\text{max}} = 665$  nm and the spectrum were plotted as C<sub>t</sub>/C<sub>0</sub> versus the irradiation time.

Similar photocatalytic setup was used in case of *E. coli* microbial removal. First, *E. coli* (ATCC 25922) bacterium was cultured in sterile LB Broth (Sigma-USA) and incubated without shaking for 12 h at 37 °C. After that, the bacterial suspension was centrifuged at 5,000g and re-suspended in fresh autoclaved LB Broth to obtain an absorbance 620 of 0.900 ± 0.05 at 600 nm. Photocatalytic setup was used to study rejection rate of bacteria using each type of fibers. *E. coli* samples were collected every one hour for total of 6 h. To determine the number of alive bacteria in samples viable cell count was used [35]. The numbers of Colony Forming Units (CFU) in 1 mL of each sample were determined by plating of 0.1 mL of 50-times diluted sample onto a Petri dish containing sterile nutrient agar (Difco, USA). The plates were incubated without shaking at 37 °C for 24 h to allow microbial growth. Then the number of colonies was counted manually and transformed into CFU/mL using the formula; CFU/mL = Number of colonies × Dilution factor/Plated volume (mL).

### 2.4. Photoluminescence measurement

In order to estimate the extent of OH<sup>·</sup> radical generation by the PES fibers under visible light excitation, PL spectra of aqueous terephthalic acid (TA) was probed by using Perkin Elmer LS55 fluorescence

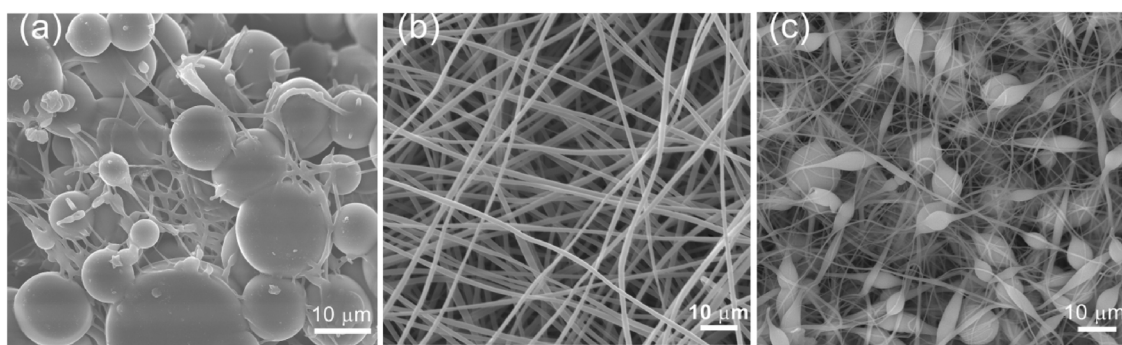


**Fig. 1.** SEM micrographs showing the morphology of the PES fibers at three different concentrations of PES fibers in 7:3 DMF/NMP mixture which were electrospun at 1.00 ml/h rate. (a) 22% PES shows particulate structure, (b) 26% PES shows uniform and smooth fibers and (c) 28% PES shows beaded fibers.

spectrometer. Excitation wavelength of 315 nm was used in all PL measurements [40]. 0.5 mM of terephthalic acid in basic media containing NaOH (2 mM) was used in this case. 30 mL of 0.5 mM terephthalic acid was added to PES fibers (3 cm × 3 cm) and kept it under light irradiation for 3 h with intensity 1000 W/m<sup>2</sup>. The emission was measured at every 15 min for total of 3 h. The same procedure was also repeated in absence of light for electrospun PES fibers and TA alone as control.

### 2.5. Filtration performance tests

Dead-end cell system (Sterlitech, HP4750) was used to perform the flux of water and bacteria media. Electrospun PES nanofibers were placed in the cell without applying any external pressure. The effective filtration area of the cell was 28.7 cm<sup>2</sup> and the levels of water and media were maintained during the experiment. The water flux was estimated by measuring the flux in mL each 15 min for total of 2 h and calculated using equation  $J = Q_p/A_m$ , Where  $J$  = flux,  $Q_p$  = filtration flow rate through the membrane (L/h) and  $A_m$  = surface area of the membrane (m<sup>2</sup>).

## 3. Results and discussion

### 3.1. PES nanofibers characterization

In order to investigate the effect of PES polymer percentages on fibers formation, three different percentages of PES were added in a mixture of DMF and NMP. The morphology of the obtained PES electrospun nanofibrous membranes with 22%, 26%, 28% of PES in 7:3 DMF:NMP mixture were then investigated using SEM as shown in Fig. 1. The morphology at 26% PES shows uniform and smooth fibers, while at 22% PES particulate structure were obtained instead of fibers and at concentration higher than 26% beaded fibers were formed. Therefore, 26% PES sample has been used here for the rest of the investigations. The ratio of DMF and NMP was previously established as shown in Table 1, where different ratios of DMF can change the physical properties of the solution such as solvent volatility polymer concentration and solvent viscosity [41]. Similar to other studies,

increasing amount of added DMF contribute in smaller fibre diameter which is mainly attributed to the higher electric conductivity, lower vapour pressure and higher dielectric constant of the solvent. [25,41]. Thinner fibers were observed at 7:3 DMF:NMP ratio with reasonably good hydrophobicity. However with increasing DMF concentrations the mechanical strength of the fibers were observed to reduce gradually, while flux was increased continuously. The SEM micrographs of fibers obtained with different ratio of DMF and NMP are shown in the supplementary data (Fig. S1).

The hydrophilicity of the fibers was further reduced in order to increase the water flux by oxidizing the fibers using ammonium persulfate [25]. Oxidation using ammonium persulfate did not change fiber diameter, as shown in Supplementary data (Fig. S2). The WCA after oxidation was reduced to 42.25°, indicating the hydrophilic nature of the fibers (Supplementary data Fig. S3). For the ammonium persulfate treated fibers the pure water flux reached up to 522.65 L/h m<sup>2</sup>.

### 3.2. Photocatalysis and photoluminescence tests

PES polymer has been reported to have both direct (~ 2.92 eV) and indirect (2.60 eV) band gaps [42], and so the PES molecule by itself could show photocatalytic property under light irradiation. Moreover, it has been reported that PES polymer can produce OH· radicals as a result of photo irradiation [37]. This means that PES nanofibers have self-cleaning properties. In order to investigate the photocatalytic activity of fabricated PES fibers, photocatalytic degradation was carried out on ISO standard model dye methylene blue (MB) under stimulated visible light [43]. The presence of OH· radicals as a consequence of photo-irradiation, initiated reactions leading to MB degradation [44]. Fig. 2 shows the course of degradation of MB with respect to its change in concentration ( $C_t/C_0$ ) upon irradiation time for both in absence (control) and in the presence of hydrophobic PES nanofibers. Under illumination condition PES fibers show more than 80% reduction in MB concentration compared to the control sample where no PES fibers was present.

To further investigate generation of OH· by PES fibers under visible light irradiation, PL measurement using terephthalic acid (TA) has been

**Table 1**

Effect of percentage of DMF in NMP as solvent mixture in PES electrospun fibers.

DMF : NMP	Fiber diameter (nm)	Mechanical strength		Contact angle (°)	Pure water flux (L/h m <sup>2</sup> )
		Ultimate strength (MPa)	Young Modulus (MPa)		
1:1	740 ± 80	4.12	71.82	143.29 ± 0.89	10.87
3:2	320 ± 20	1.71	40.15	134.52 ± 1.30	41.39
7:3	193 ± 25	0.79	14.73	126.14 ± 0.99	93.86

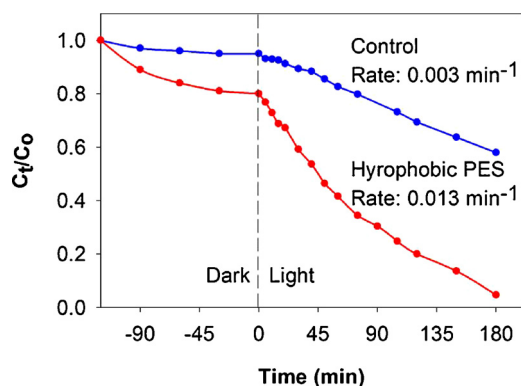


**Fig. 2.** Photocatalytic degradation of MB by hydrophobic PES nanofibers in dark and under visible light irradiation. Rate of MB degradation was determined by using first order exponential decay fitting [fitting data not shown here].

carried out. **Fig. 3a** shows the PL spectra of TA solution under visible light obtained at different time in the presence of PES. Highly fluorescent product, 2-hydroxyterephthalic acid was detected, which is a product of the chemical reaction between OH· radicals and TA during light illumination [40,45], where the source of OH· radicals is the PES fibers in this case. The PL signal at 425 nm indicated the formation of 2-hydroxyterephthalic acid compound and the intensity is proportional to the amount of OH· radical generated by PES fibers that was observed to increase continuously with time (**Fig. 3b**). In absence of PES, TA alone did not show significant increase in PL intensity at 425 nm. In absence of light, formation of OH· radicals was not observed as shown in **Fig. S4** of supplementary data. These results confirmed that PES fibers in the presence of light produces OH· radicals that can degrade organic pollutants. However with the chemically treated hydrophilic fibers, the formation of OH· radicals was found to reduce due to the chemical oxidation treatment as shown in **Fig. 3b**.

We further investigated if there is any self-destruction of the PES fibers due to the generation of highly reactive OH· radicals. The investigation was carried out by FTIR analysis to confirm any change in the functional groups of PES polymer. It appeared that there is no considerable change in the functional groups of the polymer structure as shows in **Fig. 4**. Moreover, a weak peak was observed to appear at around  $1027\text{ cm}^{-1}$  after continuous light irradiation. This new band can arise from the formation of sulfonic acid derivatives ( $\text{R}-\text{SO}_3\text{H}$ ) as a result of prolonged light illumination, as reported previously [37]. The reaction between oxygen and PES surface during light irradiation is fast

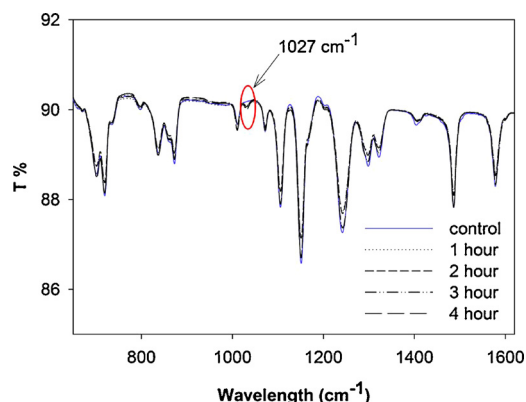


**Fig. 4.** The FTIR spectra of PES membrane before and after exposure to the light for three hours.

and non-specific, and the formation of  $-\text{SO}_3\text{H}$  group is the predominant process in this case [46]. Moreover, the amount of light dose is proportional to amount formation of this group. However, this group has no effect in photocatalytic process since  $\text{SO}_2^-$  has already reacted to form  $-\text{SO}_3\text{H}$  group [46].

### 3.3. Photocatalysis densification of *E. coli*

According to earlier studies, PES membranes modified with metal oxide nanoparticles such as  $\text{TiO}_2$  and  $\text{ZnO}$  showed inhibition of the growth of microorganism [29,47,48]. However, no previous reports showed antimicrobial activity of PES fibers alone due to photocatalysis. Here we further studied the antibacterial activities of our PES fibers against *E. coli* bacteria and the antibacterial performance was evaluated by estimating the number of viable bacterial cells (CFU). From **Fig. 5**, it was observed that, after six hours of photocatalytic treatment, hydrophilic fibers showed almost 16% reduction in colony forming units (CFU) whereas on the other hand hydrophobic PES fibers showed significantly higher reduction in colony forming units (~78%). As the observed antimicrobial effect was significantly higher in light experiment in comparison with the dark experiment where  $P > 0.05$ , the observed photocatalytic antimicrobial effect of PES fibers can be attributed to the production of hydroxyl radicals ( $\text{OH}^\cdot$ ) by PES fibers. The antimicrobial mechanism of reactive oxygen species is well known [49]. These hydroxyl radicals being extremely reactive indiscriminately attack polysaccharides, membrane lipids and membrane proteins which are essential to maintain membrane integrity in bacterial cells. Overall oxidative stress generated through the production of hydroxyl radicals

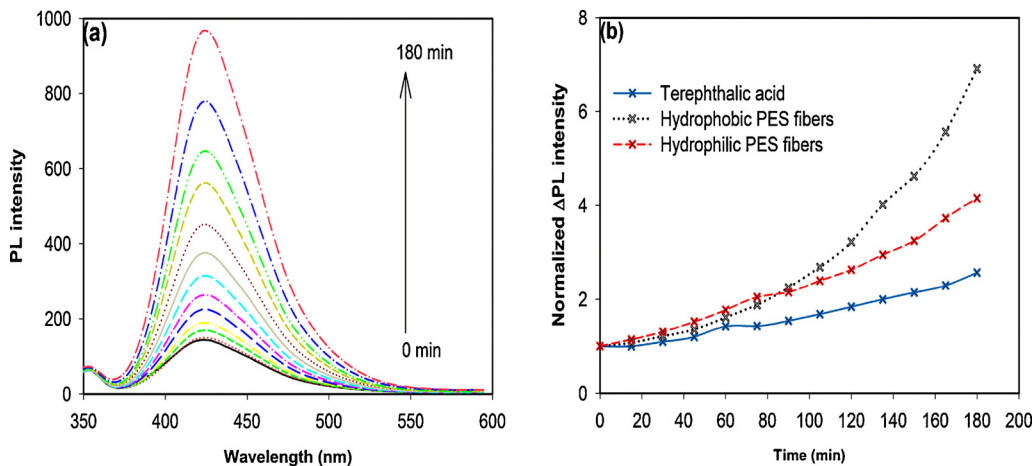


**Fig. 3.** (a) PL spectral changes under visible light irradiation with increasing time for hydrophobic PES fibers in 0.5 mM terephthalic acid, (b) PL intensity at 425 nm under visible light irradiation as a function of time for TA alone, as prepared PES fibers and chemically treated fibers.

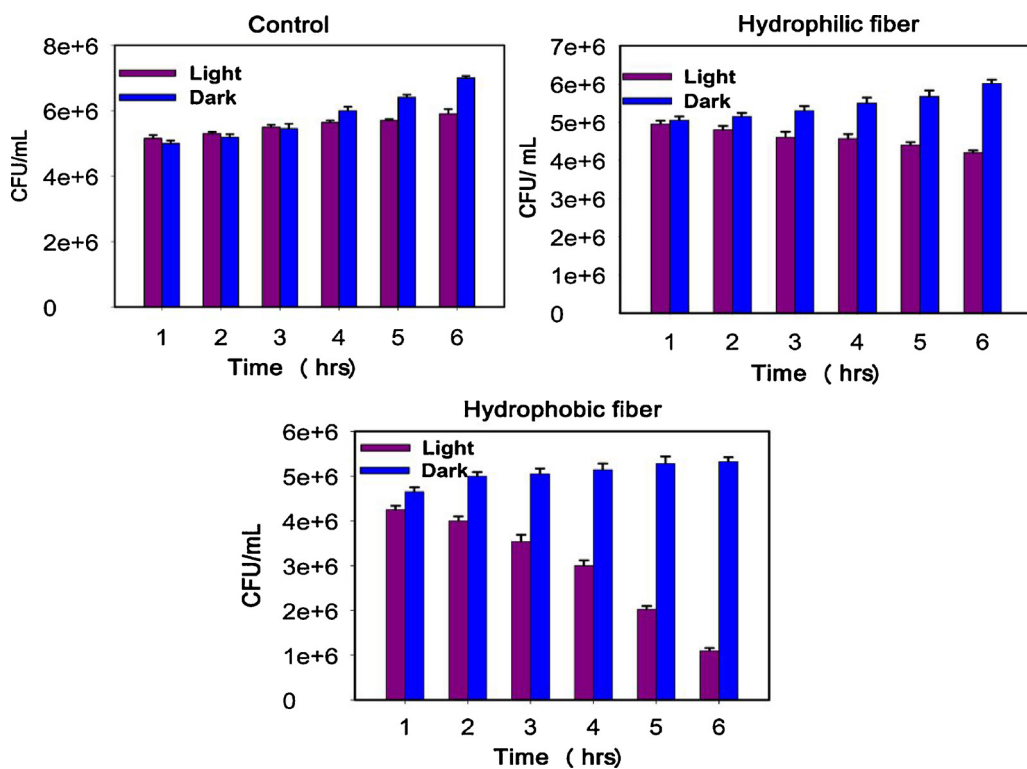


Fig. 5. Number of colonies of *E. coli* for hydrophobic and hydrophilic fibers in dark and under light condition.

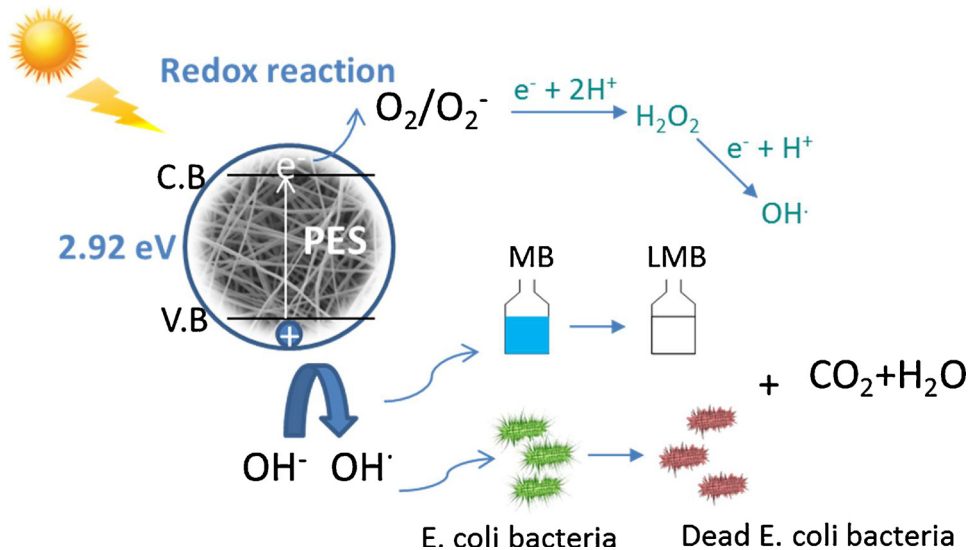


Fig. 6. Illustration showing the mechanism of photocatalytic methylene blue (MB) degradation and bacterial removal using the PES fibres.

causes *E. coli* cell death via fibers damage, lipid peroxidation and by causing structural changes in cell envelope [50]. Better performance of hydrophobic fibers over hydrophilic fibers was also evident with bacterial flux measurements. Higher antibacterial activity of the hydrophobic fibers can be explained with the several folds higher production of hydroxyl radicals compared to hydrophilic fibers as shown in Fig. 3.

According to the literatures [37,42] and photocatalysis results tests, the mechanism of photocatalysis by PES fibers can be explain as in Fig. 6.

When PES fibres are exposed with visible light, electron-hole pairs generate through bandgap absorption resulting hydroxyl radicals ( $\text{OH}^{\cdot}$ ) and superoxide radicals ( $\text{O}_2^{\cdot-}$ ). The  $\text{O}_2^{\cdot-}$  radicals can further undergo cascaded reactions with  $\text{H}^+$  and photogenerated electrons ( $e^-$ )

producing peroxides ( $\text{H}_2\text{O}_2$ ) and subsequently more  $\text{OH}^{\cdot}$  radicals. These  $\text{OH}^{\cdot}$  radicals can oxidize organic molecules and can disrupt the microbial cell wall through oxidative stress resulting in degradation of organic pollutants and microbes in water in the presence of light.

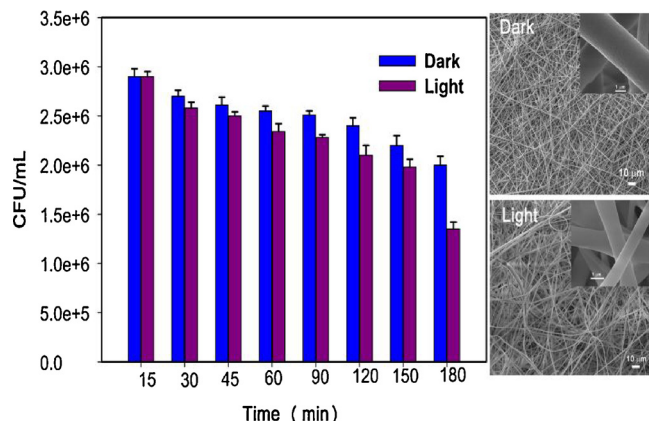
Therefore, PES fiber photocatalytic activity can be compare to others some polymer or semiconductor catalysts as shown in Table 2.

The filtration flux experiment was then conducted to investigate applicability of the electrospun fibers in water treatment. Fig. 7 shows the number of rejected bacterial by hydrophobic electrospun PES fibers in presence of light using *E. coli* as test contaminant where the flow flux was  $33.49 \text{ L/h m}^2$ . The reduction in the number of colonies could be explained by two hypothesis; 1) photocatalytic behaviour of the PES fibers and 2) accumulation of rejected bacteria on the surface of the

**Table 2**

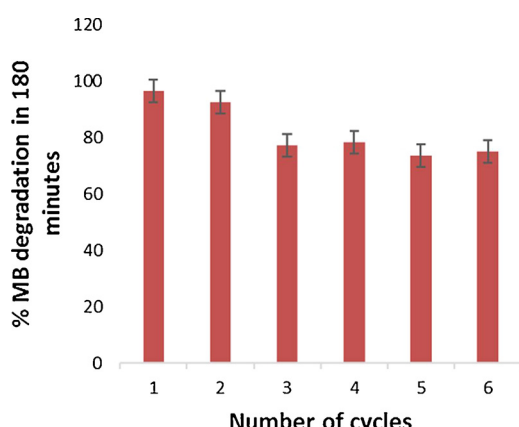
Shows photocatalytic activity comparison of some commonly used semiconductors with PES fibers.

Photocatalyst	Band gap (eV)	Photocatalytic applications	Ref
PES	2.92	Organic dye (methylene blue) and bacteria ( <i>E. coli</i> )	This work
ZnO	3.37	Oxidise organic contaminant, organic contaminants, and can cause fatal damage to microorganisms by disrupting their cell wall.	[51]
TiO <sub>2</sub> anatase	3.2	Removal of toxic potassium cyanide5	[52]
ZnS	3.54	Degrade natural organic matters photocatalytic removal of toxic Hg(II) and CH <sub>3</sub> Hg(II) chlorides	[53]
$\alpha$ -Fe <sub>2</sub> O <sub>3</sub>	2.1	Degrade Azo dye	[54]
		Photodegradation of phenol	

**Fig. 7.** Number of colonies of *E. coli* bacteria for hydrophobic fibers in dark and under light condition during filtration flux experiment.

membrane. However, SEM results (Fig. 7) revealed that no *E. coli* bacteria adsorbs to the fiber surface permanently and hence making the surface self-cleaning surface with less pore blocking effect.

To further confirm the photocatalytic stability of PES fibers, repeatable tests were carried out, the results showed in Fig. 8 and found that the photocatalytic performance of the fibres initially drops (about 20%) when repeated for 3 times. However, after 3 cycles, the performance remained almost unchanged and consistently showed ~78% reduction in MB concentrations after 180 min when repeated for another 3 times. Currently we are investigating strategies to improve the stability of the fibres and therefore the stability results are not included in the present manuscript.

**Fig. 8.** Repeatability test of PES fibres against MB solution. PES fibers were washed with 5% HCl in Methanol in between the repeated cycles [55]. MB concentration in terms of % after 180 min of photocatalytic degradation is presented.

#### 4. Conclusion

Nanofibers of electrospun PES polymer were successfully prepared by using higher percentage of highly-volatile DMF and lower percentages of NMP as solvents. The average fibers diameter was decreased almost 3.8 times by increasing the percentage of DMF. Therefore, it contributes in the increasing the surface to volume ratio and decreases the water barriers in water application. However, the mechanical strength of the fibers was reduced due to the lower percentages of NMP, where NMP increase the adhesion between fibers. The amount of PES polymer during the growth of the fibers was also found to be crucial for the formation of fiber structure, where lower amount of PES resulted in no fiber formation while excess PES exhibited beaded fibers. PL and FTIR studies revealed that under visible light illumination PES can be a source of OH<sup>·</sup> radicals leading to improved photocatalytic degradation of organic dyes, as well as effective bacterial growth inhibitor. By changing the surface chemistry through oxidation to make the fibers more hydrophilic resulted in improvement in water flux, however reduced their ability to produce OH<sup>·</sup> radicals. The photocatalytic nature of the PES fibers therefore gives the surface a self-cleaning property which will surely have a great impact in future membrane design technology.

#### Acknowledgements

The authors would like to thank the Chair in Nanotechnology, The Research Council of Oman for the financial support to carry out this research work. SD work was supported by TRC [RC/AGR/FISH/16/01] and internal SQU [IG/AGR/FISH/15/02] grants.

#### Appendix A. Supplementary data

Supplementary material related to this article can be found, in the online version, at doi:<https://doi.org/10.1016/j.apcatb.2018.03.095>.

#### References

- [1] M. Paul, S.D. Jons, Chemistry and fabrication of polymeric nanofiltration membranes: a review, *Polymer* 103 (2016) 417–456.
- [2] G. Mannella, V. La Carrubba, V. Brucato, Some features of polymeric membranes for water purification via membrane distillation, *J. Appl. Polym. Sci.* 122 (2011) 3557–3563.
- [3] M. Kabsch-Korbutowicz, A. Urbanowska, Comparison of polymeric and ceramic ultrafiltration membranes for separation of natural organic matter from water, *Environ. Prot. Eng.* 36 (2010) 125–135.
- [4] M.M. Pendergast, E.M. Hoek, A review of water treatment membrane nano-technologies, *Energy Environ. Sci.* 4 (2011) 1946–1971.
- [5] B.S. Lalia, V. Kochkodan, R. Hashaikeh, N. Hilal, A review on membrane fabrication: structure, properties and performance relationship, *Desalination* 326 (2013) 77–95.
- [6] S.S. Ray, S.-S. Chen, C.-W. Li, N.C. Nguyen, A comprehensive review: electrospinning technique for fabrication and surface modification of membranes for water treatment application, *RSC Adv.* 6 (2016) 85495–85514.
- [7] M. Ulbricht, Advanced functional polymer membranes, *Polymer* 47 (2006) 2217–2262.
- [8] S.S. Homaeigohar, K. Buhr, K. Ebert, Polyethersulfone electrospun nanofibrous composite membrane for liquid filtration, *J. Membr. Sci.* 365 (2010) 68–77.

[9] A. Ghaee, M. Shariati-Niassar, J. Barzin, A. Ismail, Chitosan/polyethersulfone composite nanofiltration membrane for industrial wastewater treatment, *Int. J. Nanosci. Nanotechnol.* 9 (2013) 213–220.

[10] A. Frenot, I.S. Chronakis, Polymer nanofibers assembled by electrospinning, *Curr. Opin. Colloid Interface Sci.* 8 (2003) 64–75.

[11] B. Kwankhao, *Microfiltration Membranes via Electrospinning of Polyethersulfone Solutions*, Universität Duisburg-Essen, Fakultät für Chemie, 2013.

[12] H. Rezaei, F.Z. Ashtiani, A. Fouladitajar, Fouling behavior and performance of microfiltration membranes for whey treatment in steady and unsteady-state conditions, *Braz. J. Chem. Eng.* 31 (2014) 503–518.

[13] B. Ladewig, M.N.Z. Al-Shaiei, *Fundamentals of membrane bioreactors: materials, Systems and Membrane Fouling*, Springer, 2016.

[14] Z. Li, C. Wang, Effects of working parameters on electrospinning, *One-Dimensional Nanostructures*, Springer, 2013, pp. 15–28.

[15] S. Wong, An Investigation of Process Parameters to Optimize the Fiber Diameter of Electrospun Vascular Scaffolds Through Experimental Design, (2010).

[16] X. Wang, C. Drew, S.-H. Lee, K.J. Senecal, J. Kumar, L.A. Samuelson, Electrospun nanofibrous membranes for highly sensitive optical sensors, *Nano Lett.* 2 (2002) 1273–1275.

[17] H. Abdallah, A. El-Gendi, M. Khedr, E. El-Zanati, Hydrophobic polyethersulfone porous membranes for membrane distillation, *Front. Chem. Sci. Eng.* 9 (2015) 84–93.

[18] L.Y. Ng, A. Ahmad, A.W. Mohammad, Alteration of polyethersulphone membranes through UV-induced modification using various materials: a brief review, *Arab. J. Chem.* (2013).

[19] H.Q. Dang, L.D. Nghiem, W.E. Price, Factors governing the rejection of trace organic contaminants by nanofiltration and reverse osmosis membranes, *Desalination Water Treat.* 52 (2014) 589–599.

[20] C. Bellona, J.E. Drewes, P. Xu, G. Amy, Factors affecting the rejection of organic solutes during NF/RO treatment—a literature review, *Water Res.* 38 (2004) 2795–2809.

[21] K.L. Tu, A.R. Chivas, L.D. Nghiem, Effects of membrane fouling and scaling on boron rejection by nanofiltration and reverse osmosis membranes, *Desalination* 279 (2011) 269–277.

[22] M. Peyravi, A. Rahimpour, M. Jahanshahi, A. Javadi, A. Shockravi, Tailoring the surface properties of PES ultrafiltration membranes to reduce the fouling resistance using synthesized hydrophilic copolymer, *Microporous Mesoporous Mater.* 160 (2012) 114–125.

[23] N. Maximous, G. Nakhl, W. Wan, K. Wong, Effect of the metal oxide particle distributions on modified PES membranes characteristics and performance, *J. Membr. Sci.* 361 (2010) 213–222.

[24] R. Singh, *Membrane Technology and Engineering for Water Purification: Application, Systems Design and Operation*, Butterworth-Heinemann, 2014.

[25] K. Yoon, B.S. Hsiao, B. Chu, Formation of functional polyethersulfone electrospun membrane for water purification by mixed solvent and oxidation processes, *Polymer* 50 (2009) 2893–2899.

[26] A.W. Mohammad, I.N.H.M. Amin, Fouling of Ultrafiltration Membrane During Adsorption of Long Chain Fatty Acid in Glycerine Solutions, (2013).

[27] T. Nguyen, F.A. Roddick, L. Fan, Biofouling of water treatment membranes: a review of the underlying causes, monitoring techniques and control measures, *Membranes* 2 (2012) 804–840.

[28] K. Rasool, D.S. Lee, Inhibitory effects of silver nanoparticles on removal of organic pollutants and sulfate in an anaerobic biological wastewater treatment process, *J. Nanosci. Nanotechnol.* 16 (2016) 4456–4463.

[29] P. Sathe, J. Richter, M.T.Z. Myint, S. Dobretsov, J. Dutta, Self-decontaminating photocatalytic zinc oxide nanorod coatings for prevention of marine microfouling: a mesocosm study, *Biofouling* 32 (2016) 383–395.

[30] Leaf-nosed bat, *Encyclopædia Britannica*, Encyclopædia Britannica Online, 2009.

[31] E. Igbinigun, Y. Fennell, R. Malaisamy, K.L. Jones, V. Morris, Graphene oxide functionalized polyethersulfone membrane to reduce organic fouling, *J. Membr. Sci.* 514 (2016) 518–526.

[32] X. Yang, J. Qin, Y. Jiang, K. Chen, X. Yan, D. Zhang, R. Li, H. Tang, Fabrication of P25/Ag 3 PO 4/graphene oxide heterostructures for enhanced solar photocatalytic degradation of organic pollutants and bacteria, *Appl. Catal. B: Environ.* 166 (2015) 231–240.

[33] M.M. Khan, S.F. Adil, A. Al-Mayouf, Metal oxides as photocatalysts, *J. Saudi Chem. Soc.* 19 (2015) 462–464.

[34] A.M. Al-Hamdi, M. Sillanpää, J. Dutta, Photocatalytic degradation of phenol by iodine doped tin oxide nanoparticles under UV and sunlight irradiation, *J. Alloys Compd.* 618 (2015) 366–371.

[35] P. Sathe, M.T.Z. Myint, S. Dobretsov, J. Dutta, Removal and regrowth inhibition of microalgae using visible light photocatalysis with ZnO nanorods: a green technology, *Sep. Purif. Technol.* 162 (2016) 61–67.

[36] D. Zhao, G. Sheng, C. Chen, X. Wang, Enhanced photocatalytic degradation of methylene blue under visible irradiation on graphene@TiO 2 dyade structure, *Appl. Catal. B: Environ.* 111 (2012) 303–308.

[37] K. Norrman, P. Kingshott, B. Kaeleby, A. Ghanbari-Siahkali, Photodegradation of poly (ether sulphone) part 1. A time-of-flight secondary ion mass spectrometry study, *Surf. Interface Anal.* 36 (2004) 1533–1541.

[38] J.J. Foti, B. Devadoss, J.A. Winkler, J.J. Collins, G.C. Walker, Oxidation of the guanine nucleotide pool underlies cell death by bactericidal antibiotics, *Science* 336 (2012) 315–319.

[39] M.D. Labas, C.S. Zalazar, R.J. Brandi, A.E. Cassano, Reaction kinetics of bacteria disinfection employing hydrogen peroxide, *Biochem. Eng. J.* 38 (2008) 78–87.

[40] Y. Liu, C. Liu, J. Wei, R. Xiong, C. Pan, J. Shi, Enhanced adsorption and visible-light-induced photocatalytic activity of hydroxyapatite modified Ag-TiO 2 powders, *Appl. Surf. Sci.* 256 (2010) 6390–6394.

[41] N. Nuraje, W.S. Khan, Y. Lei, M. Ceylan, R. Asmatulu, Superhydrophobic electrospun nanofibers, *J. Mater. Chem. A* 1 (2013) 1929–1946.

[42] Siddhartha, S. Aarya, M. Shakir, A.K. Srivastava, M.A. Wahab, Morphological, electrical, structural and optical properties of Co60 gamma rays irradiated polyethersulfone (PES) polymer, *Int. J. Phys. Appl.* 3 (1) (2011) 16.

[43] T. Bora, P. Sathe, K. Laxman, S. Dobretsov, J. Dutta, Defect engineered visible light active ZnO nanorods for photocatalytic treatment of water, *Catal. Today* 284 (2017) 11–18.

[44] T. Bora, M. Myint, S. Al-Harthi, J. Dutta, Role of surface defects on visible light enabled plasmonic photocatalysis in Au-ZnO nanocatalysts, *RSC Adv.* 5 (2015) 96670–96680.

[45] J.-C. Sin, S.-M. Lam, K.-T. Lee, A.R. Mohamed, Photocatalytic performance of novel samarium-doped spherical-like ZnO hierarchical nanostructures under visible light irradiation for 2, 4-dichlorophenol degradation, *J. Colloid Interface Sci.* 401 (2013) 40–49.

[46] K. Norrman, F.C. Krebs, Photodegradation of poly (ether sulphone) part 2. Wavelength and atmosphere dependence, *Surf. Interface Anal.* 36 (2004) 1542–1549.

[47] Z.-X. Low, Z. Wang, S. Leong, A. Razmjou, L.F. Dumée, X. Zhang, H. Wang, Enhancement of the antifouling properties and filtration performance of poly (ethersulfone) ultrafiltration membranes by incorporation of nanoporous titania nanoparticles, *Ind. Eng. Chem. Res.* 54 (2015) 11188–11198.

[48] S. Pigeot-Rémy, F. Simonet, E. Errazuriz-Cerda, J. Lazzaroni, D. Atlan, C. Guillard, Photocatalysis and disinfection of water: identification of potential bacterial targets, *Appl. Catal. B: Environ.* 104 (2011) 390–398.

[49] M. Cho, H. Chung, W. Choi, J. Yoon, Linear correlation between inactivation of *E. coli* and OH radical concentration in TiO 2 photocatalytic disinfection, *Water Res.* 38 (2004) 1069–1077.

[50] E. Cabisco, J. Tamarit, J. Ros, Oxidative stress in bacteria and protein damage by reactive oxygen species, *Int. Microbiol.* 3 (2010) 3–8.

[51] R.J. Barnes, R. Molina, J. Xu, P.J. Dobson, I.P. Thompson, Comparison of TiO 2 and ZnO nanoparticles for photocatalytic degradation of methylene blue and the correlated inactivation of gram-positive and gram-negative bacteria, *J. Nanopart. Res.* 15 (2013) 1432.

[52] O. Ola, M.M. Maroto-Valer, Review of material design and reactor engineering on TiO2 photocatalysis for CO2 reduction, *J. Photochem. Photobiol. C: Photochem. Rev.* 24 (2015) 16–42.

[53] M. El-Kemary, H. El-Shamy, Fluorescence modulation and photodegradation characteristics of safranin O dye in the presence of ZnS nanoparticles, *J. Photochem. Photobiol. A: Chem.* 205 (2009) 151–155.

[54] M. Valenzuela, P. Bosch, J. Jiménez-Becerrill, O. Quiroz, A. Páez, Preparation, characterization and photocatalytic activity of ZnO, Fe2O3 and ZnFe2O4, *J. Photochem. Photobiol. A: Chem.* 148 (2002) 177–182.

[55] A. Celebioglu, Z.I. Yildiz, T. Uyar, Electrospun crosslinked poly-cyclodextrin nanofibers: highly efficient molecular filtration thru host-guest inclusion complexation, *Sci. Rep.* 7 (2017) 7369.